

Catalytic and Physical Properties of Phosphorus-Modified ZSM-5 Zeolite

JACQUES C. VÉDRINE,¹ ALINE AUROUX, PIERRE DEJAIFVE,² VALENTIN DUCARME, HANNA HOSER,³ AND SHUIBAO ZHOU⁴

Institut de Recherches sur la Catalyse (CNRS), 2 Avenue Albert Einstein, 69626-Villeurbanne Cédex, France

Received April 6, 1981; revised September 9, 1981

H-ZSM-5 zeolite modified by phosphorus (1.1 and 2.0 wt%) was studied by means of infrared spectroscopy and microcalorimetry for acidity characterization, by ESCA for determining elementary composition in the outer layers (depth $\approx 50 \text{ \AA}$) with respect to the bulk ($\phi \approx \text{several } \mu\text{m}$), and lastly by catalytic reaction analysis of methanol conversion. It was found that phosphorus neutralizes acidic sites primarily at the entrance of the channels of the zeolite particles in the same manner as do carbonaceous residues after some time of reaction. However, the strongest acid sites remain unmodified, which leads to the suggestion that the aluminium distribution and subsequently the acid site strength distribution along the zeolite channels is heterogeneous. Phosphorus-modified zeolites gave a higher yield of light olefins ($C_2^- - C_4^-$) and subsequently a smaller yield of saturated aliphatics and aromatics than the parent zeolite in the methanol conversion reaction. The phosphorus-modified zeolite gave similar yields of the *meta* + *para* isomers of xylene and of ethyltoluene and a smaller yield of the *ortho* isomers. Lastly the yield of heavier aromatics A_6^+ was greatly decreased by the addition of phosphorus. The changes in selectivity were tentatively assigned to slight modifications in channel size and to increased tortuosity due to phosphorus compounds bonding to the zeolite framework, rather than to changes in acid strength.

INTRODUCTION

Increasing interest has recently been focussed on the transformation of methanol to compounds which commercially are highly desirable, and in this connection a novel class of zeolites, designated ZSM, exhibiting very valuable and fascinating properties of shape selectivity, has been developed (1, 2). These solids also have the important property of retaining their crystallinity for long periods of time in spite of the presence of steam at high temperature. Moreover, the formation of carbonaceous deposits is very low (3, 4), resulting in very

long times on stream between burning regenerations, which can be performed at higher than usual temperatures.

Such properties seem surprising at first glance because of the high silica-to-alumina ratio, i.e., the low concentration of framework aluminium and associated atoms responsible for catalytic activity. These properties are due (5, 6) to the crystal structure of the channels, which provides constrained access by virtue of having a pore dimension of about 5.5 \AA from 10-membered rings of oxygen atoms.

A process has recently been developed for selectively producing xylenes by alkylating toluene with methanol (7) without forming the side products ethylbenzene and mesitylene, which need to be separated by expensive fractionation and multistage refrigeration steps. This process also favors formation of *para*-xylene with respect to *ortho*-xylene and, to a greater extent, with respect to *meta*-xylene, the latter being the least commercially desired product. The

¹ To whom queries concerning this paper should be sent.

² Present address: Laboratoire de Recherches, Shell Recherche S.A., 76530 Grand Couronne, France.

³ Permanent address: Institute of Organic Chemistry, Polish Academy of Sciences, ul. Kasprzaka 44, 01-224 Warsaw, Poland.

⁴ Permanent address: Laboratory of Catalysis, Chemistry Department, Nankai University, Tianjin, China.

most preferred process is to modify the ZSM zeolite by the addition of a Group Va element, e.g., phosphorus, arsenic, or antimony. The amount added to the zeolite should be at least 0.5 and preferably 2 to 15% by weight. The effect of the additive element is to limit formation of aromatics from methanol (7). It was suggested (7, 8) that changes in selectivity are due to the incorporation of the Group Va element, which provides the catalyst with a greater number of acid sites but of lesser strength than the parent zeolite. Moreover, modification of zeolite channels may also occur, changing the accessibility to reactants (9).

The purpose of the present work was to use infrared spectroscopy and calorimetry to characterize the acidity of phosphorus-modified ZSM zeolite, to use ESCA to determine if phosphorus really enters the zeolite pores, and subsequently to follow the change in catalytic selectivity of the material in the reaction of methanol conversion. The amount of phosphorus added was specially kept low in order to follow more precisely the effect of introducing a foreign compound, since with high phosphorus contents the probability that some of the phosphorus atoms do not play any role in the catalytic modification is obviously enhanced.

EXPERIMENTAL

Catalysts

The H-ZSM-5 zeolite samples were prepared according to the procedure described previously (10). Acidification was performed four times by a treatment with NH_4Cl solutions at 80°C and the crystallinity was checked by X-ray diffraction.

Modification with phosphorus was performed following two different procedures. To obtain sample A_2 , phosphorus was added to an acidified A_1 sample following a procedure described in Ref. (7). The zeolite A_2 was flushed under nitrogen at 230°C , then treated in a trimethylphosphite solu-

tion in *n*-octane for 16 hr at 120°C . The sample was filtered, washed with *n*-pentane, methylene chloride, and *n*-pentane, dried in air then under vacuum at 110°C overnight, and heated in air flow at 540°C for 3 hr. To avoid any loss of acidity or activity, which could occur due to methanol from the decomposition of trimethylphosphite, the sample was rehydrated under water vapor at 80°C for 4 hr, at 100°C for 2 hr, and then heated under air flow at 550°C for 16 hr. To obtain sample B_2 from sample B_1 (Na form), phosphorus was added following the same procedure as above but before acidification. After heating the phosphorated material at 540°C under air flow, acidification was carried out classically with NH_4Cl aqueous solution at 80°C for four times and the ammonium ions were decomposed under air flow at 540°C . The elemental composition of the samples is given in Table 1.

Materials

The methanol was high-purity reagent grade (99+%), used without further purification. Ammonia, for acidity characterization in infrared spectroscopy and microcalorimetry, was supplied by Air Liquide, dried over Na wire, and deoxygenated by the freeze-pump-thaw technique.

Catalytic Apparatus and Procedure

The conversion reaction was performed using about 0.1 g of catalyst placed in a fixed-bed continuous-flow Pyrex reactor. The vapor phase of the thermostated liquid reagent was carried through the catalytic bed using nitrogen as carrier gas, monitored to obtain a weight hourly space velocity around $10\text{--}12\text{ hr}^{-1}$. The experimental procedure is described in more detail in Ref. (11).

Physical Methods

Microcalorimetric measurements were

TABLE 1
Chemical Analysis of Elemental Composition of ZSM-5 Zeolite Samples

Sample	Designation	Chemical analysis*			Chemical formula (taking Si + Al = 96 per u.c.)	SiO ₂ Al ₂ O ₃ (mol%)
		Na	Al	P		
A ₁	H-ZSM-5	0.27	4	—	Na _{0.7} H _{7.8} Al _{8.5} Si _{87.5} O ₁₉₂	20.5
A ₂	P-HZSM-5	0.27	4.2	1.1	Na _{0.7} H _{6.6} P _{2.1} Al _{9.3} Si _{88.7} O ₁₉₂	18.6
B ₁	H-ZSM-5	0.30	3.2	—	Na _{0.8} H _{6.4} Al _{7.5} Si _{88.5} O ₁₉₂	24.7
B ₂	P-HZSM-5	0.43	3.3	2.0	Na _{1.1} H _{6.2} P _{3.9} Al _{7.3} Si _{88.7} O ₁₉₂	24.3

* element contents in wt %

performed with a heat flow microcalorimeter maintained at 150°C. Procedures of calibration and of ammonia adsorption by successive pulses have been described previously (12). Before the calorimetric experiments, the samples were evacuated overnight at 400°C down to a pressure of 10⁻⁴ Torr in order to eliminate molecular water.

Infrared spectroscopy measurements were performed using a Perkin-Elmer 580 spectrometer. Thin wafers of roughly 10 mg were outgassed overnight at 400°C to obtain maximum Brønsted acidity (13). The spectra were recorded at room temperature.

Scanning electron micrographs were taken with a Jeol electron microscope. ESCA studies were carried out after outgassing the sample at room temperature (10⁻⁸ Torr) in a HP 5950 A Hewlett-Packard spectrometer monitored by computer. The ESCA lines were smoothed and subtracted from the background. Their relative areas were determined by means of a com-

puter. Because of a broad line under the Al_{2s} line due to phonons of the Si_{2p} line, particularly for these low-Al: Si-ratio zeolites, we chose the Al_{2p} line for the quantitative determination of the Al content.

RESULTS AND DISCUSSION

ESCA Data

Samples A and B were studied with AlK α monochromatized X-ray photons at

TABLE 2

Binding Energy Values (in eV) for Different Elements of ZSM-5 Zeolite Samples (± 0.2 eV) after Charging Effect Correction: Si_{2s} at 154.0 eV (14)

Samples	XPS lines					
	Na _{1s}	O _{1s}	P _{2s}	P _{2p_{3/2}}	Si _{2p}	Al _{2p}
A ₂	1072.5	532.4	191.8	134.5	102.9	74.5
B ₂	1072.4	532.4	191.7	134.5	102.9	74.5

TABLE 3

Structure and Binding Energy Values for Phosphorus Compounds^a

Compounds	E _B
P ^{red}	130.1
P PH ₃	131.9
P Bz ₃	130.6
P (oEt) ₃	133.0
O=P Ph ₃	132.9
O=P Bz ₃	132.7
O=P(oEt)Et ₂	133.1
O=P(OH)Ph ₂	133.5
O=P(OH) ₂ Bz	133.8
O=P(OEt) ₃	134.2
O=P(OBz) ₃	134.2
O=P(OPh) ₃	134.9
Na ₃ PO ₄	132.1
K ₂ H PO ₄	132.7
KH ₂ PO ₄	133.9

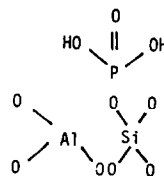
^a Energies in electron volts. P_{2p_{3/2}} lines from Ref. (15) and therein.



FIG. 1. Scanning electron micrographs of phosphorated samples A (A) and B (B). The white horizontal bar represents 1 μm .

room temperature without heat treatment in the spectrometer. The binding energy values reported in Table 2 may be compared to those given in Table 3 for different phosphorus compounds as a function of the number and nature of the attached ligands. Although such values have to be taken into account with particular care because of the charging effect, one can reasonably conclude by comparison that elemental phosphorus bonds to the zeolite framework

through oxygen as suggested by Kaeding and Butter (8) and schematized below:



with P in the 5+ oxidation state.

Table 4 reports quantitative atomic ratios



FIG. 1.—Continued.

determined chemically and by ESCA for the different elements of samples A and B. Although such determinations are rather imprecise in ESCA ($\pm 20\%$), the good agreement we have obtained in the case of Y-type zeolite (14) between ESCA and chemical analysis data leads us to conclude that for sample B the Si:Al ratio is higher at the surface layers of the zeolite particles than in the bulk but for sample A the Si:Al ratio is the same. The former result could indicate an inhomogeneous distribution of

aluminium atoms within the zeolite particles with surface layers poorer in aluminium, while the latter result suggests that such inhomogeneity depends on the synthesis conditions. The same conclusion could also be drawn from synthesis studies by Chen *et al.* (17), and was further suggested by Derouane *et al.* (18) and by von Ballmoos and Meier (19). On the other hand, this inhomogeneity was not observed by Suib *et al.* (20) from Auger electron spectroscopy studies.

ESCA data also clearly show that the P content is two to three times larger within the first layers of the zeolite particles, say within about 50 Å, than in the bulk for sample A and similar between surface and bulk for sample B. It could also have been possible that the P compound was only deposited at the surface of the particles, i.e., was not entering the zeolite channels. However, in such a case on the basis of a rough calculation assuming spherical particles of 2 μm diameter and using the approximate relationship (21) $n/n_0 = (3\lambda/4r^3)(r^2 - \lambda^2/12)$, one could expect an atomic P: (Si + Al) ratio equal to $(2.1/0.2) \times (96/100) \approx 10$ instead of 0.05 for sample A and ≈ 20 instead of 0.04 for sample B. n and n_0 are respectively the number of atoms as detected by ESCA and by chemical analysis, r the radius of the particle, and λ the mean free path of the corresponding electron ($\lambda \approx 20$ Å presently). It follows that one can reasonably conclude that phosphorus enters the zeolite channels and neutralizes the acid framework hydroxyl groups at the channel entrance and along the interior of the channels, proportionally to the phosphorus amount (which remains much less than the Al content). It follows that the surface phosphorus concentration, as measured by ESCA, is higher than the total when the Al concentration is similar be-

tween the surface and the bulk (sample A). In sample B the phosphorus concentration, as measured by ESCA and chemical analysis, is the same in the surface and the bulk. However, this is purely coincidental since the concentration of aluminium, to which the phosphorus is indirectly attached, is smaller near the surface than in the bulk. It follows that the P content coincidentally corresponds to the overall P concentration with respect to Si + Al.

Scanning Electron Microscopy Data

The particles observed in SEM photographs correspond to irregular spherical particles for sample A (0.2 to 2 μm in diameter) and to regular parallelepipeds for sample B (0.2–0.5 wide, 1–3 μm long) as shown in Fig. 1. Amorphous parts of the samples were not observed.

Infrared Data

The infrared spectra in the regions 1300–1600 and 3300–3800 cm⁻¹ are shown in Fig. 2. It is clear that the 3730- and 3605-cm⁻¹ OH bands (13) are present in all samples with a much lower intensity for both lines in the case of P-modified zeolites. Moreover, the adsorption of ammonia on Brønsted sites gives ammonium ion bands at 3375 and 1465 cm⁻¹ which disappear for all sam-

TABLE 4

Comparison between Quantitative Chemical Analysis ($\pm 3\%$) and ESCA Data ($\pm 20\%$) in Atomic Ratios of the Elements of ZSM-5 Zeolites Samples

Samples	Si: Al		(Si + Al): O ESCA	P: (Si + Al)		Na: (Si + Al)	
	Chemical analysis	ESCA		Chemical analysis	ESCA	Chemical analysis	ESCA
A ₁	10.2	9	0.5	—	—	0.007	0.03
A ₂	9.3	10	0.5	0.02	0.05	0.007	0.08
B ₁	12.8	17	0.4	—	—	0.008	0.005
B ₂	12.6	18	0.5	0.04	0.04	0.012	0.020

Note. Quantitative ESCA ratios are calculated from the corresponding peak area ratios using the approximate relationship: $n_1/n_2 = (A_1/A_2)(E_k^{1/2} \sigma_2/E_k^{1/2} \sigma_1)$, where E_k refers to the kinetic energy of the level and σ to its cross section as given by Schofield (16).

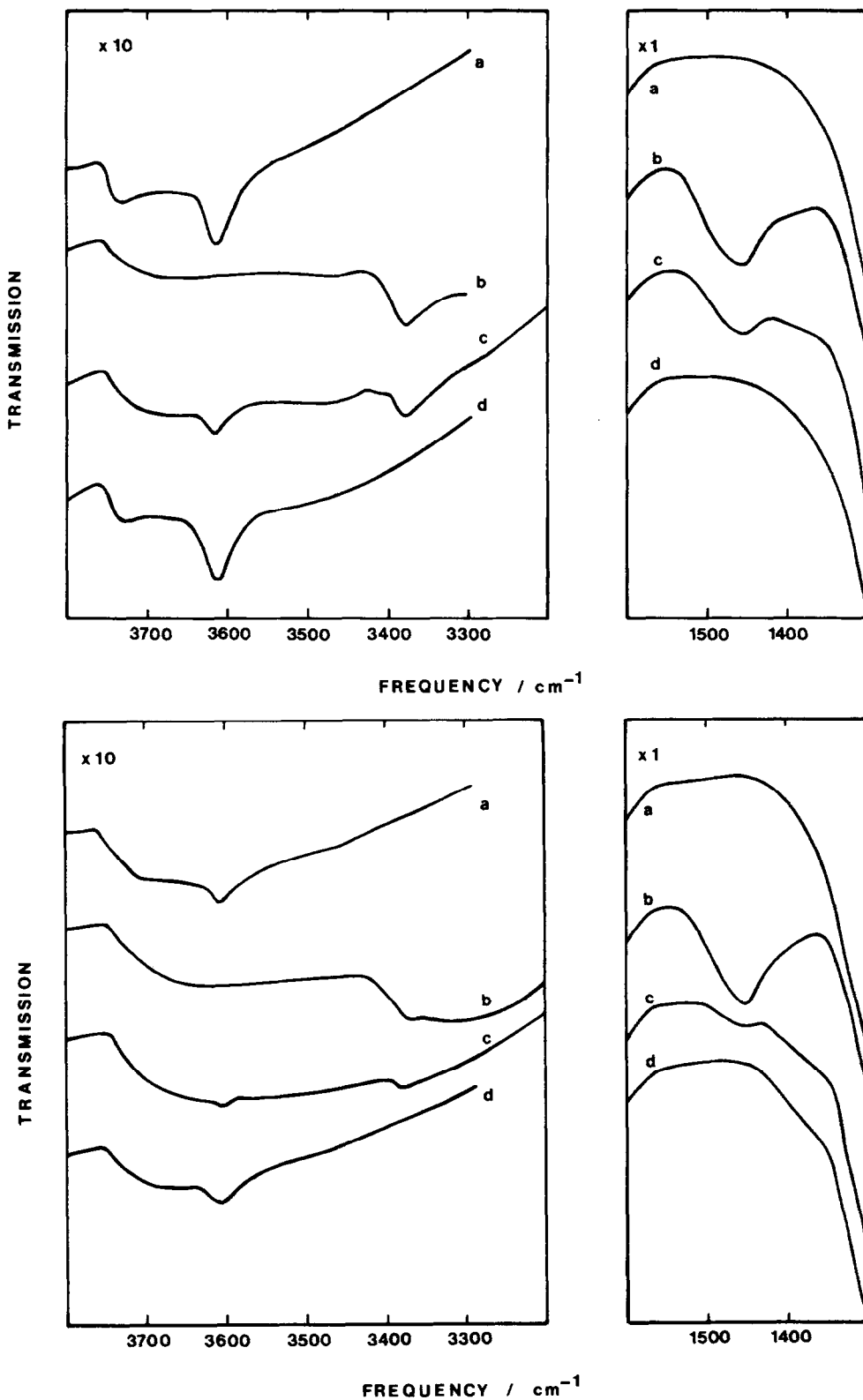


FIG. 2. Infrared spectra in the regions 3300–3800 and 1300–1600 cm⁻¹ observed for H-ZSM-5 (A₁ top) and P-ZSM-5 (A₂ bottom) samples. Spectrum a corresponds to samples outgassed at 400°C, b to samples a after NH₃ adsorption at 150°C and outgassing at room temperature, c to samples b outgassed at 150°C, and d to samples c outgassed at 200°C. The wafers were of the same weight.

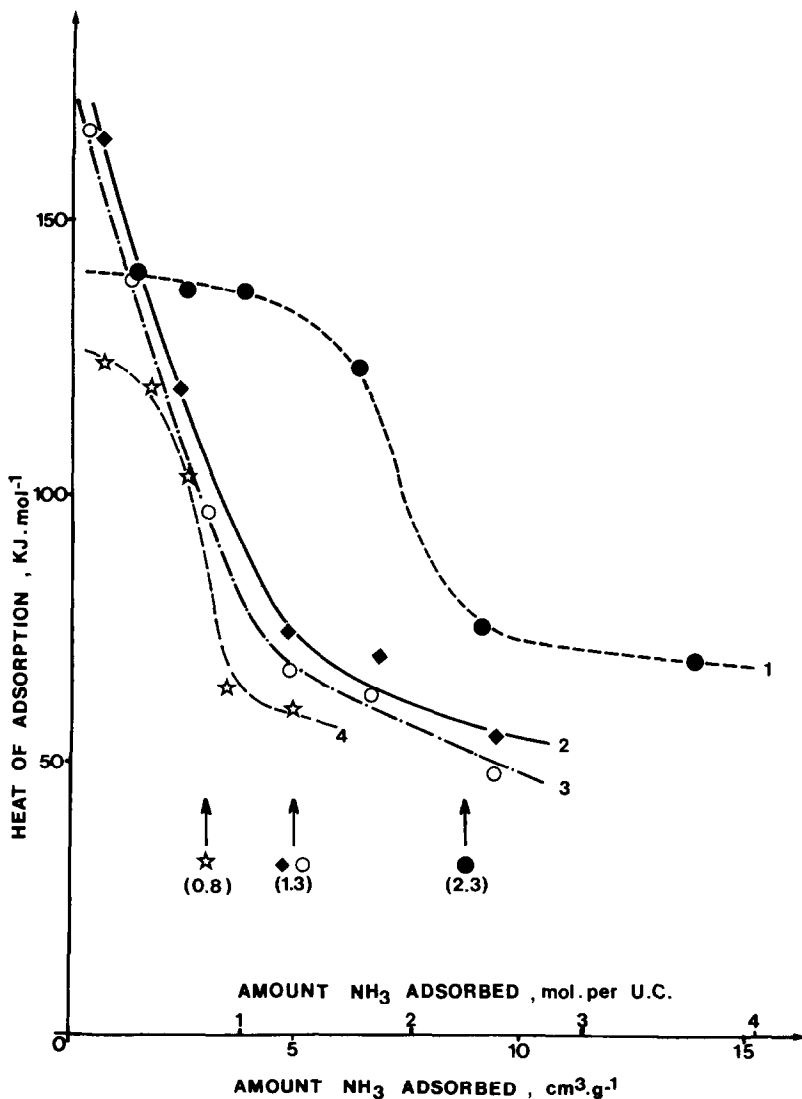


FIG. 3. Heat of adsorption at 150°C as a function of ammonia coverage for samples outgassed at 400°C overnight. 1: H-ZSM-5 sample (A_1). 2: P-ZSM-5 sample (A_2). 3: Sample A_1 after 20 min methanol conversion at 370°C and outgassing at 400°C. 4: Sample A_2 treated as in 3. The arrows and the corresponding values in parentheses correspond to the strongest NH_3 adsorption extent in mol per u.c. and can be compared to the number of protons from chemical analysis (7.8 and 6.6. per u.c. for samples A_1 and A_2 , respectively).

ples by outgassing between 150 and 200°C. It may then be concluded that phosphorus has neutralized a large part of the acidic OH groups but the strength of the remaining acid sites is still comparable to that of the parent zeolite as far as the infrared technique and thermodesorption measurements

can tell. A large value in NH_4^+ ir band intensity at 1465 and 3300–3380 cm^{-1} for P-modified zeolite may arise from the action of NH_3 on OH groups of the phosphorated compound (see the scheme above), OH groups which are not detected by infrared because of H-bond broadening.

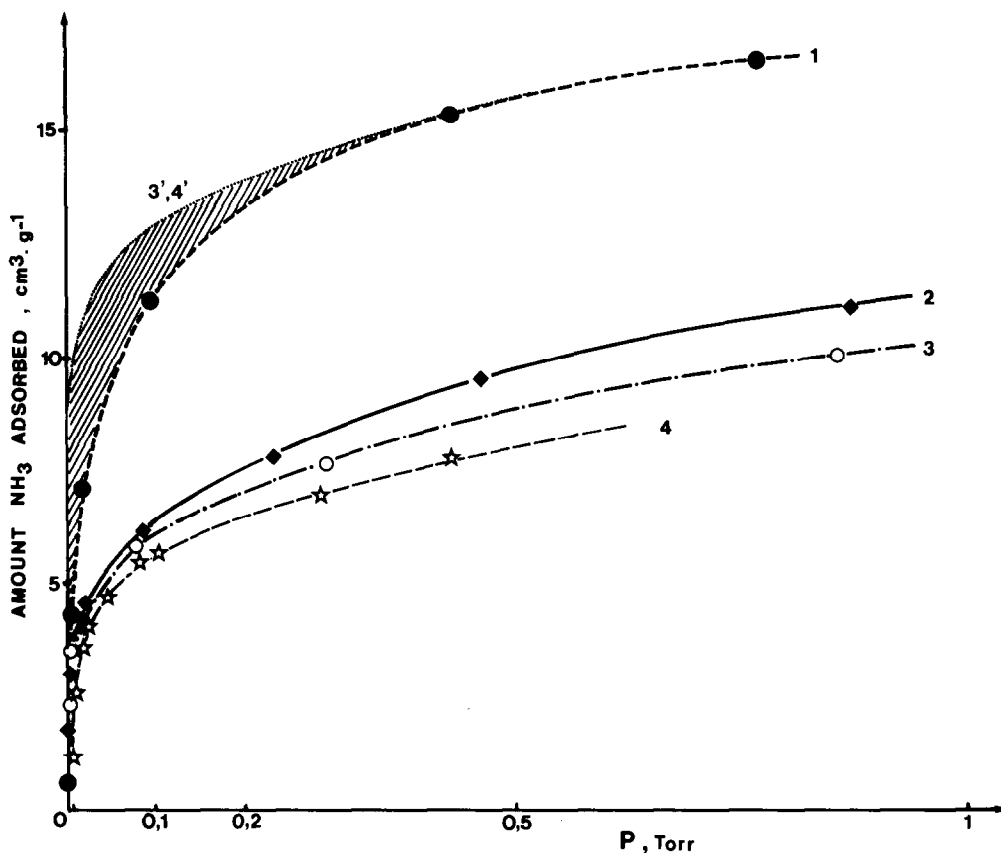


FIG. 4. Isotherms of NH_3 adsorption for samples 1 to 4 described in the caption to Fig. 3. The shaded area corresponds to the difference between the isotherm curve obtained for the H-ZSM-5 samples and that obtained for the P-modified sample but vertically translated to superposition at high NH_3 coverage. This shaded area represents the changes in the amount of medium acid strength due to phosphoration (4).

Microcalorimetric Data

Successive pulses of ammonia were introduced at 150°C on the four samples previously outgassed at 400°C overnight. The heats of ammonia adsorption were measured with a heat flow microcalorimeter maintained at 150°C . The variations of the heats of adsorption as a function of the successive pulses are presented in Figs. 3 and 5 and the adsorption isotherms are given in Fig. 4. It is clear (4) that the number of acid sites has drastically decreased (roughly by 60%) by phosphoration but the strongest acid sites are still present. Further, even stronger acid sites seem to exist, which

in our opinion is due to the fact that the calorimetry method measures an "average" strong acid strength value. Indeed we have shown previously (12) that due to the constrained access to the acid site along the zeolitic channels, ammonia neutralizes first the acid sites close to the channel openings which may be of lesser strength than inner sites. This very probably arises from a heterogeneous Al distribution along the channel, since it has been shown that acid strength of Brønsted sites in zeolite matrices decreases with the concentration of aluminium (22). The "average" strong acid strength, as measured by microcalorimetry, was shown to remain about constant in a

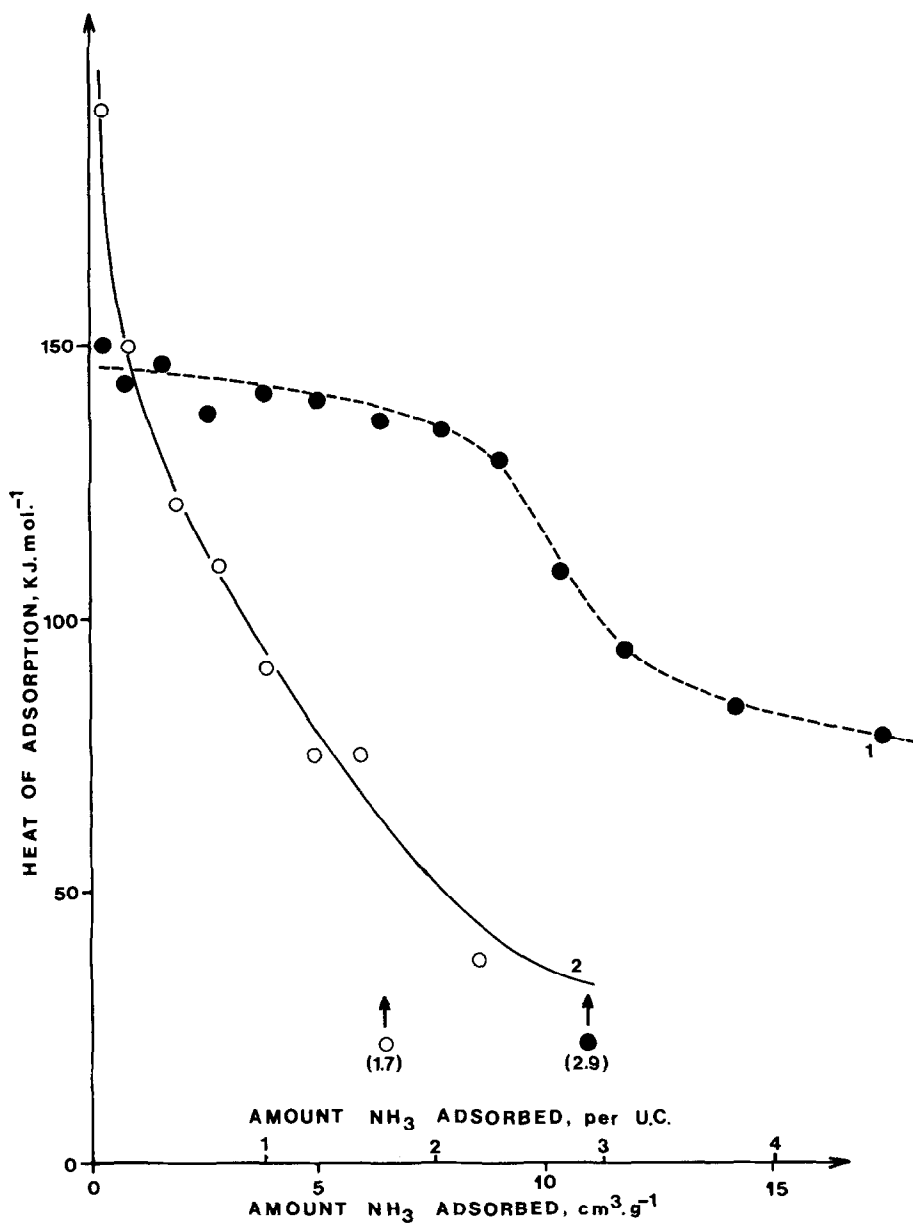


FIG. 5. Heat of adsorption at 150°C as a function of ammonia coverage for samples B outgassed at 400°C overnight. 1: H-ZSM-5 sample (B₁). 2: P-ZSM-5 sample (B₂).

broad domain of Al content (23). All these observations are consistent with a model of heterogeneous acid strength distribution along the channels with particularly the strongest sites being innermost (18). The phosphorus compound neutralizes first the outer strong acid sites of the channels while

the inner and strongest acid sites are not modified. Changes in microcalorimetric curve response were not observed when phosphorus was added as could be expected if more constraint existed. This presumably stems from the lengthy response of the Calvet calorimeter which can only

TABLE 5

Conversion of Methanol to Hydrocarbons over Acidic and Phosphorus-Modified ZSM-5 Zeolite: Sample A

	Samples					
	A ₁			A ₂ (P: 1.1 wt%)		
Reaction conditions						
WHSV (hr ⁻¹)	11.7	11.8	11.9	12.1	12.4	11.2
Temperature (°C)	370	420	470	370	420	470
Conversion (wt%)	89	92	79	89	92	93
CH ₃ OCH ₃	4	3.5	11	5	5	3
CH ₃ OH	7	4.5	12	5	3	5
Weight percentages						
Hydrocarbons						
Aliphatics	67	71	76	84	90	90
Aromatics	33	29	24	16	10	10
Olefins						
C ₂ ⁻	13	12	13	18	14	13
C ₃ ⁻	21	26	29	29	37	40
C ₄ ⁻	10	11	12	14	17	17
C ₂ ⁻ -C ₄ ⁻ (total)	44	49	54	61	68	70
C ₅ ⁻ -C ₇ ⁻	8	8	10	12	12	12
Paraffins						
C ₃ -C ₉ ⁺	15	14	12	11	10	8
Aromatics						
Benzene	0.3	0.3	0.3	0.4	0.4	0.5
Toluene	1.8	2.0	1.5	0.8	0.6	0.7
(<i>m</i> + <i>p</i>)-Xylene	15	13	11	10	6	6.5
<i>o</i> -Xylene	1.5	1.5	1.5	0.3	0.3	0.5
1,2,4-Trimethylbenzene	6	5.5	5	0.6	0.5	0.4
(<i>m</i> + <i>p</i>)-Ethyltoluene	4	3	2	2	1	0.8
<i>o</i> -Ethyltoluene + 1,3,5-trimethylbenzene	0.1	0.1	0.2	—	—	—
A ₉ ⁺	4.6	3.6	2.9	1.9	1.2	0.6
Selectivity						
(<i>m</i> + <i>p</i>): <i>o</i> -Xylene	11	9	8	35	18	13
(<i>m</i> + <i>p</i>): <i>o</i> -Ethyltoluene	56	26	13	∞ ^a	∞ ^a	∞ ^a

^a *o*-Ethyltoluene was not detected.

give average values rather than instantaneous ones.

It is also worthy of note that carbonaceous residues obviously formed at the outer acid sites of the particles in the methanol conversion reaction lead to a similar effect on acid sites, as shown in Fig. 3. Figure 3 also shows that the strongest acid sites are only neutralized for samples modified both by the phosphorus compound and by carbonaceous residues, but a strong acidity still remains.

Catalytic Data in the Methanol Conversion Reaction

Comparison of the activity and selectivity of samples A and B and their phosphorated homologues in the methanol conversion reaction is presented in Tables 5 and 6 after 20 min of reaction. The main features may be summarized as follows.

(i) The activity of phosphorus-modified zeolite is roughly similar to that of the parent sample.

TABLE 6

Conversion of Methanol to Hydrocarbons over Acidic and Phosphorus-Modified ZSM-5 Zeolite: Sample B

	Samples					
	B ₁			B ₂ (P: 2.0%)		
Reactions conditions						
WHSV (hr ⁻¹)	12.4	12.3	12.4	12.4	12.3	12.1
Temperature (°C)	370	420	470	370	420	470
Conversion (wt%)	78	88	86	75	88	83
CH ₃ OCH ₃	16	6	7	17	5	11
CH ₃ OH	6	6	7	8	7	6
Weight percentages						
Hydrocarbons						
Aliphatics	72	71	68	81	85	89
Aromatics	28	28	32	19	15	11
Olefins						
C ₂ ⁼	13	12	11	19	14	13
C ₃ ⁼	24	26	26	29	35	40
C ₄ ⁼	12	12	12	12	16	18
C ₂ ⁼ -C ₄ ⁼ (total)	49	50	49	60	65	71
C ₅ ⁼ -C ₇ ⁼	9	9	9	11	11	10
Paraffins						
C ₃ -C ₈ ⁺	14	12	10	10	9	8
Aromatics						
Benzene	0.5	0.5	0.5	0.5	0.5	1
Toluene	2	2.5	2	1	1	1
(<i>m</i> + <i>p</i>)-Xylene	9.5	11	13	10.5	9	6.5
<i>o</i> -Xylene	1	1.5	1.5	0.3	0.3	0.2
1,2,4-Trimethylbenzene	6	6	7	1	1	1
(<i>m</i> + <i>p</i>)-Ethyltoluene	3	2	2	2.5	1.5	1
<i>o</i> -Ethyltoluene + 1,3,5-trimethylbenzene	0.2	0.2	0.3	—	—	0.05
A ₉ ⁺	5.8	5.3	5.7	3.2	1.7	0.25
Selectivity						
(<i>m</i> + <i>p</i>): <i>o</i> -Xylene	10	8	8	39	27	34
(<i>m</i> + <i>p</i>): <i>o</i> -Ethyltoluene	16	11	7	∞ ^a	∞ ^a	20

^a *o*-Ethyltoluene was not detected.

(ii) The yield of light olefins (C₂⁼-C₄⁼) is greatly increased by phosphoration in agreement with the findings of Kaeding and Butter (8).

(iii) The yield of aromatics and subsequently of paraffins is greatly decreased, particularly for 1,2,4-trimethylbenzene, *o*-xylene, and heavier aromatics (A₉⁺), while the yield of (*m* + *p*)-xylene is slightly diminished. This means an increase in the (*m* + *p*):*o* ratios for xylenes and ethyltoluenes, i.e., a better shape selectivity which

we assign to an enhanced tortuosity (24) due to the attached phosphorus compounds (see the last two lines in Tables 5 and 6).

(iv) The effect of the temperature of methanol conversion reaction is also reported in Tables 5 and 6. The percentage of aromatization is generally decreased by increasing temperature but in general the product distributions are only slightly modified except for light olefins C₂⁼-C₄⁼, particularly the propene, and for the phosphorus-modified zeolite.

CONCLUSIONS

The present work shows that phosphorus-modified zeolite presents catalytic properties in the methanol conversion reaction different from those of the parent zeolite. The increase in light-olefin yield and the subsequent decrease in aromatics and saturated aliphatics formation was previously interpreted (8) as due to an increase in the number of acid sites but a decrease in their strength in the material due to phosphorus reaction with acidic hydroxyl groups. However, our study using infrared and microcalorimetry techniques clearly indicates that phosphorus neutralizes medium and strong acid sites mainly at the entrance of the zeolite channels, but does not modify the strongest acid sites. The latter sites have been shown to correspond to low Al content and to be localized in the inner part of the zeolite channels. Our data have allowed us to conclude that there is a heterogeneous distribution of aluminium atoms along the zeolite channels, with a smaller Al concentration within the zeolite particle and a heterogeneity which greatly depends on the synthesis conditions (18). This also explains the wide acidity distribution of such ZSM zeolite samples with respect to other acidic zeolites such as Y or mordenite types (12).

Although the structure of P-modified zeolite remains partly speculative at present, the changes in catalytic selectivity in the methanol conversion reaction may in our opinion be due to slight changes in the size of the channels (i.e., a more constrained access, and increased tortuosity) and to the neutralization of a part of the acidic sites rather than to a decrease in the strength of the acid sites responsible for the catalytic reaction. This conclusion is also supported by the fact that in ZSM-5 zeolite certain particles, containing aluminium-free zeolitic shells on their surface (25) or with increased tortuosity due to inorganic salt or coke plugging (26), have been observed to give an unusually high yield of *para*-xylene with respect to the *ortho* and *meta* isomers.

ACKNOWLEDGMENTS

The help of Dr. M. Primet for infrared characterization is gratefully acknowledged. We also thank M. Fassiotte for taking scanning electron micrographs at the Laboratoire des Matériaux Organiques (Solaize). One of us (P.D.) would like to acknowledge fellowships from CNRS and NATO. The authors are also grateful to Drs. E. G. Derouane, P. C. Gravelle, and C. Naccache for valuable discussions.

REFERENCES

1. Argauer, R. J., and Landolt, G. R., U.S. Patent 3,702,886 (1972).
2. Chang, C. C., and Silvestri, A. J., *J. Catal.* **47**, 249 (1977) and U.S. Patent 3928483 (1975).
3. Rollmann, L. D., and Walsh, D. E., *J. Catal.* **56**, 139 (1979).
4. Dejaifve, P., Auroux, A., Gravelle, P. C., Védrine, J. C., Gabelica, Z., and Derouane, E. G., *J. Catal.* **70**, 123 (1981).
5. Weisz, P. B., in "Proceedings, 7th International Congress on Catalysis, Tokyo, 1980" (T. Seiyama and K. Tanabe, Eds.), p. 3. Elsevier, Amsterdam, 1981.
6. Derouane, E. G., and Védrine, J. C., *J. Mol. Catal.* **8**, 479 (1980).
7. Butter, S. A., and Kaeding, W. W., U.S. Patents 3,965,208 and 3,972,832 (1976); Kaeding, W. W., Chu, C., Young, L. B., Weinstein, B., and Butter, S. A., *J. Catal.* **67**, 159 (1981).
8. Kaeding, W. W., and Butter, S. A., *J. Catal.* **61**, 155 (1980).
9. Chen, N. Y., Kaeding, W. W., and Dwyer, F. J., *J. Amer. Chem. Soc.* **101**, 6783 (1979).
10. Derouane, E. G., B. Nagy, J., Dejaifve, P., van Hooff, J. H. C., Spekman, B. P., Védrine, J. C., and Naccache, C., *J. Catal.* **53**, 40 (1978).
11. Dejaifve, P., Védrine, J. C., Bolis, V., and Derouane, E. G., *J. Catal.* **63**, 331 (1980).
12. Auroux, A., Bolis, V., Wierzchowski, P., Gravelle, P. C., and Védrine, J. C., *J. Chem. Soc. Faraday Trans. 2* **75**, 2544 (1979).
13. Védrine, J. C., Auroux, A., Bolis, V., Dejaifve, P., Naccache, C., Wierzchowski, P., Derouane, E. G., B. Nagy, J., Gilson, J. P., van Hooff, J. H. C., van den Berg, J. P., and Wolthuizen, J., *J. Catal.* **59**, 248 (1979).
14. Védrine, J. C., Dufaux, M., Naccache, C., and Imelik, B., *J. Chem. Soc. Trans. 1* **74**, 440 (1978).
15. Pelavin, M., Hendrickson, D. N., Hollander, J. M., and Jolly, W. L., *J. Phys. Chem.* **74**, 1116 (1970); Blackburn, J. R., Nordbeg, R., Stevie, F., Albridge, R. G., and Jones, M. M., *Inorg. Chem.* **9**, 2374 (1970); Lindberg, B. J., and Hedman, J., *Chem. Scr.* **7**, 155 (1975).
16. Scofield, J. H., *J. Electron Spectrosc.* **8**, 129 (1976).

17. Chen, N. Y., Miale, J. N., and Reagan, W. J., U.S. Patent 4,112,056 (1978).
18. Derouane, E. G., Detremmerie, S., Gabelica, Z., and Blom, N., *Appl. Catal.* **1**, 201 (1981); Derouane, E. G., Gilson, J. P., Gabelica, Z., Mousty-Desbuquoit, C., and Verbist, J. *J. Catal.* **71**, 447 (1981).
19. Von Ballmoos, R., and Meier, W. M., *Nature* **289**, 782 (1981).
20. Suib, S. L., Stucky, G. D., and Blattner, R. J., *J. Catal.* **65**, 174 (1980).
21. Védérine, J. C., Hollinger, G., and Tran Minh Duc, *J. Phys. Chem.* **82**, 1515 (1978).
22. Mortier, W. J., *J. Catal.* **55**, 138 (1978).
23. Auroux, A., Gravelle, P. C., Védérine, J. C., and Rekas, M., in "Proceedings, 5th Intern. Confer. Zeolites, Naples, 1980" (L. V. Rees, Ed.), Hayden, p. 433. London, 1980.
24. Derouane, E. G., Dejaifve, P., Gabelica, Z., and Védérine, J. C., *Faraday Discuss. R. Soc. Chem.*, **72**, in press.
25. Rollmann, L. D., U.S. Patent 4,148,713 (1979).
26. Haag, W. O., and Olson, D. H., U.S. Patent 4,117,026 (1979).